Continuous Emulsion Polymerization of Styrene in a Single Couette–Taylor Vortex Flow Reactor

XUE WEI, HIROSHI TAKAHASHI, SYUZAEMON SATO, MAMORU NOMURA

Department of Materials Science and Engineering, Fukui University, Fukui, Japan

Received 4 April 2000; accepted 28 July 2000

ABSTRACT: The effect of the geometrical and operational parameters on the mixing characteristics of a Couette–Taylor vortex flow reactor (CTVFR) were investigated and were correlated with the same parameters by using the tank-in-series model. Continuous emulsion polymerization of styrene was conducted at 50°C in a CTVFR to clarify the effects on kinetic behavior and reactor performance of operational parameters such as rotational speed of inner cylinder (Taylor number), reactor mean residence time, and emulsifier and initiator concentrations in the feed streams. It was found that steady-state monomer conversion and particle number could be freely varied only by varying the Taylor number. In order to explain the observed kinetic behavior of this polymerization system, a mathematical model was developed by combining the empirical correlation of the mixing characteristics of a CTVFR and a previously proposed kinetic model for the continuous emulsion polymerization of styrene in continuous stirred tank reactors connected in series (CSTRs). On the basis of these experimental results, it was concluded that a CTVFR is suitable for the first reactor (prereactor) of a continuous emulsion polymerization reactor system. © 2001 John Wiley & Sons, Inc. J Appl Polym Sci 80: 1931–1942, 2001

Key words: Key words: styrene; Taylor vortex flow; mixing characteristics; continuous reactor, continuous emulsion polymerization; emulsion polymerization

INTRODUCTION

Most commercial continuous emulsion polymerization processes consist of continuous stirred tank reactors connected in series (CSTRs). Because of this, many researchers have published experimental and theoretical articles on continuous emulsion polymerization in CSTRs.[1–10] Nomura et al.[6] conducted continuous emulsion polymerization of styrene in CSTRs and demonstrated experimentally and theoretically that the first CSTR serves exclusively as a particle nucleation reactor (seeder) and that even in an optimal CSTR at the highest the number of polymer particles produced is only 57% of that produced in an ideal plug flow reactor (PFR) or in a batch reactor. In order to increase the efficiency and productivity of the whole reactor system, based on this study's results, they recommended the placing of a continuous tubular reactor upstream of the CSTRs (prereactor concept), although in practice perhaps it would not work as an ideal plug flow reactor.[11]

As stated above, a continuous tubular prereactor is much more efficient in particle nucleation than is a CSTR operated under any conditions. However, this prereactor has a potential disadvantage in that plugging of the reactor tube often

Correspondence to: M. Nomura.

Journal of Applied Polymer Science, Vol. 80, 1931–1942 (2001)

takes place during long-term operation because, for example, of the deposition of flocculated polymer particles onto the reactor surface. Therefore, in practice an optimal CSTR is recommended as the prereactor, although it is less efficient in particle nucleation than is a continuous tubular prereactor. Even with a CSTR, however, fouling is experienced sometimes because of massive coagulation of latex particles induced by excessive mechanical shear caused by stirring. To avoid these defects, therefore, Imamura and Nomura[12] selected a Couette–Taylor vortex flow reactor (CTVFR) as an alternative; to investigate its characteristics as a continuous emulsion polymerization reactor, they carried out continuous seeded emulsion polymerization of styrene in a single CTVFR at 50°C. In addition, from their experimental investigation of the mixing characteristics of a CTVFR, they demonstrated that a CTVFR could be operated very close to an ideal PFR if the reactor was properly designed and was operated near the critical Taylor number.

Catalytic chemical reactors,[13] plant cell bioreactors,[14] and emulsion polymerization[12,15] are some of the practical applications of CTVFRs that have been presented over the years. Design, scale-up, and optimization for CTVFRs require a detailed understanding of the transport properties of Taylor–Couette flow. Some of these properties, such as mass and heat transfer to the cylinder walls, have been well described in the literature, while the mixing characteristics in a CTVFR have received scant attention.[16–20] The current study, therefore, had several aims: first, to investigate the mixing characteristics of a CTVFR in more detail and to empirically correlate them with the geometric and operational parameters of the reactor; then, to carry out the continuous nonseeded emulsion polymerization of styrene in a single CTVFR at 50°C in order to demonstrate experimentally that a CTVFR has the characteristics suitable for the prereactor of a continuous emulsion polymerization reactor system; and finally to further develop a mathematical model that could quantitatively explain the reactor performance and kinetic behavior observed in this polymerization system by applying a kinetic model proposed previously for the continuous emulsion polymerization of styrene in CSTRs[6] and the tank-in-series model to a CTVFR.

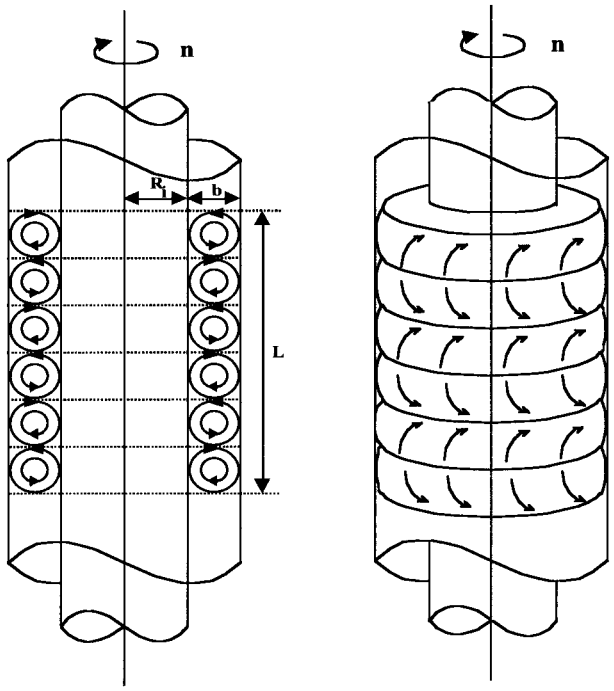

Figure 1 Schematic diagram of Couette–Taylor vortex flow.

Mixing Characteristics of a CTVFR

Figure 1 shows typical flow pattern in a CTVFR caused by the rotation of the inner of two concentric cylinders. It is well known that the flow pattern is governed by the dimensionless number called the Taylor number, Ta, defined by

$$Ta = \left(\frac{bR_i\omega}{v}\right)\left(\frac{b}{R_i}\right)^{1/2} \quad (1)$$

where R_i is the radius of the inner cylinder, b is the radial clearance between two concentric cylinders, v is the kinematics viscosity, and ω is the angular velocity of the inner cylinder. When the Taylor number exceeds a certain value between 46 and 60, called the critical Taylor number, Ta_c, a transition occurs from pure Couette flow to a flow regime in which toroidal vortices are regularly spaced along the cylinder axis, which is the so-called Couette–Taylor vortex flow.

In this article we describe the mixing characteristics of a CTVFR with the tank-in-series model that has only one parameter, N, the number of tanks connected in series. This allowed us to quantify the deviation of its flow pattern from plug flow and to correlate the model parameter,

Table I Dimensions of CTVFRs Used in This Study

Reactor Length L (cm)	Inner Cylinder Outside Diameter D_i (cm)	Outer Cylinder Inside Diameter D_o (cm)	Ratio $r = D_i/D_o$ r [−]	Number of Vortices N_0
30.5	3.80	5.0	0.434	50
30.5	3.20	5.0	0.540	34
30.5	2.70	5.0	0.640	26
30.5	2.17	5.0	0.760	22
27	2.70	4.5	0.600	30

N, with such geometric and operational parameters as reactor length, L; the diameters of inner and outer cylinders, D_i and D_o; the ratio, $r = D_i/D_o$; the number of vortices, N_o; the Taylor number, Ta; and the reactor mean residence time, θ. The number of vortices was determined by visual inspection and was found to be almost equal to the value of L/b. The geometrical parameters of several CTVFRs used for these experiments are shown in Table I. The experimental procedure and the treatment of experimental data were the same as those described previously.[12] We used the stimulus–response method to determine the value of the parameter N. All the experimental results obtained in the experiments are plotted in Figure 2 with N/N_o as ordinate and $kTa^{-2}\theta^{-1}$ as abscissa, where $k = 10^{(-6.7r^2+4r+5.05)}$. The relationship between two nondimensional variables, N/N_o and $Ta^{-2}\theta^{-1}$ can be correlated by the expression.

$$N/N_0 = 10^{(-6.7r^2+4r+6.65)}Ta^{-2}\theta^{-1} \quad (2)$$

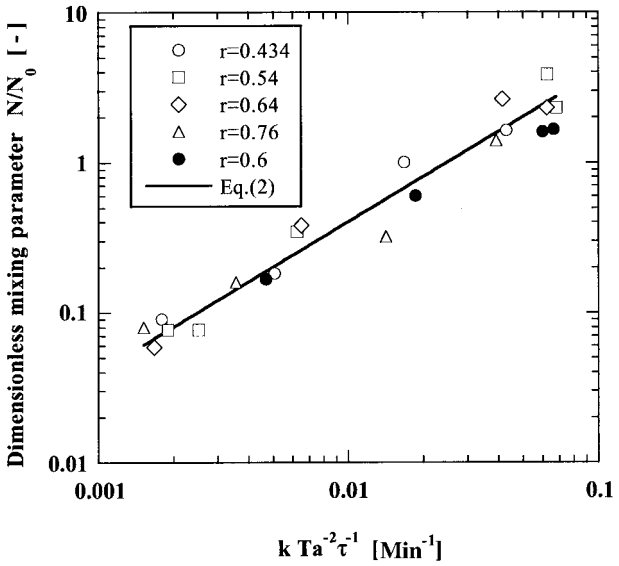

Figure 2 Correlation of dimensionless mixing parameter with geometrical and operational parameters.

EXPERIMENTAL

Continuous Emulsion Polymerization in a CTVFR

Experimental Procedure and Materials Used

Continuous emulsion polymerization of styrene was carried out in a single CTVFR consisting of an inner circular cylinder made of stainless steel and an outer circular cylinder made of glass with a water jacket. The reactor configuration is shown in detail in Figure 3. The outside diameter of the inner cylinder is 27 mm, and the inside diameter of the outer cylinder is 45 mm. The length of the reactor and the total volume of annular space are 270 mm and 292.2 cm^3, respectively. The experimental setup is shown in Figure 4. Aqueous initiator solution and monomer emulsion were held separately in individual glass-made tanks and were fed into the reactor through an inlet attached at the bottom of the reactor with each metering pump. The reaction temperature was kept constant at 50±0.5°C by circulating cooling water from a thermostated water bath through the reactor jacket. Prior to start-up, any remaining oxygen in the whole reactor system was removed by bubbling high-purity nitrogen gas (purity > 99.995%) from the reactor inlet for about 1.5 h. Then the polymerization was initiated by feeding both the monomer emulsion and the aqueous initiator solution with each metering pump to the empty reactor. Effluent reaction mixtures from the outlet attached at the top of the reactor were regularly collected and were measured for

monomer conversion and the number of polymer particles produced. Monomer conversion was determined gravimetrically using methanol as precipitant for polystyrene. The number of polymer particles produced was determined by using the monomer conversion and the volume average diameter measured by an electron microscope.

Commercial styrene monomer (Wako Pure Chemical Industries, Ltd.) was washed with 15% aqueous potassium hydroxide solution to remove inhibitor, was further washed with distilled–deionized (DDI) water several times to remove the residual base, and was then distilled under vacuum (40°C, 15–20 mmHg). DDI water was also the water used in the polymerization experiments. Potassium persulfate (Wako Pure Chemical Industries, Ltd.) and sodium lauryl sulfate (Nakarai-tesuta Co.), both analytical grade, were used as initiator and emulsifier, respectively. All the polymerization experiments were conducted in a high-purity nitrogen atmosphere.

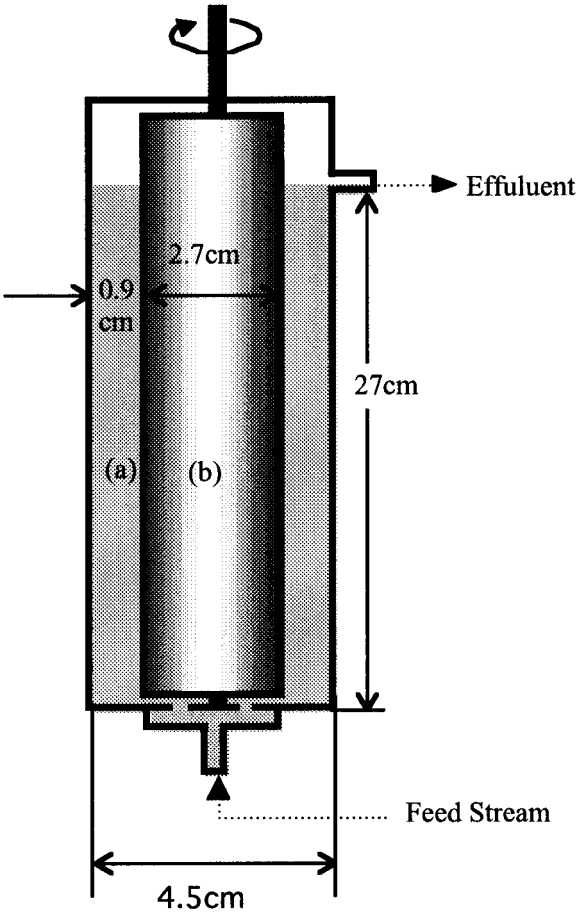

Figure 3 Schematic diagram of Couette–Taylor vortex flow reactor and its dimensions: (a) annular space of two concentric cylinders and (b) inner cylinder.

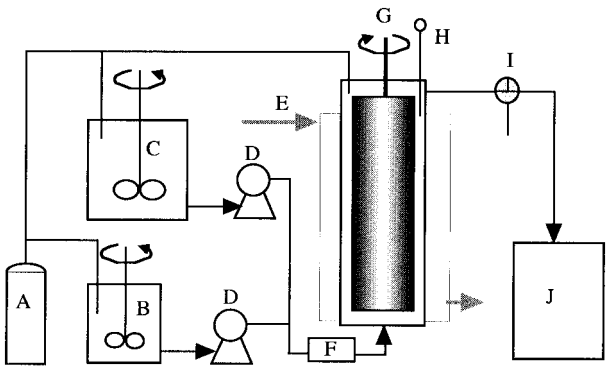

Figure 4 Schematic diagram of experimental apparatus: (A) high purity nitrogen tank, (B) storage tank for aqueous initiator solution, (C) storage tank for styrene emulsion, (D) metering pumps, (E) cooling water, (F) thermostated water bath, (G) rotational inner cylinder, (H) thermometer, (I) sampling cock, and (J) storage tank for waste emulsion.

Typical Example of Continuous Emulsion Polymerization of Styrene in a Single CTVFR

Preliminary experiments were conducted with the emulsifier and monomer concentrations in the emulsion feed stream fixed at $S_F = 6.25$ g/dm^3 of water and $M_F = 100$ g/dm^3 of water, respectively, and the initiator concentration in the initiator feed stream was set at $I_F = 1.25$ g/dm^3 of water. The rotational speed of the inner cylinder was changed in the course of polymerization. The reactor mean residence time was kept at $\theta = 21.3$ min. When this residence time was adopted, the monomer emulsion was fed at a rate of 12.5 g/min and the aqueous initiator solution at a rate of 1.26 g/min. Figure 5 shows typical examples of the monomer conversion–versus–time (dimensionless reaction time, t/θ) histories observed when the rotational speed of the inner cylinder was changed during polymerization. Figure 5(a) indicates the case where the rotational speed was first fixed at 290 rpm and then lowered to 20 rpm 205 min after the start of polymerization where the monomer conversion had already reached a steady-state value. Figure 5(b), on the other hand, shows the case where the rotational speed was changed from 145 rpm to 30 rpm. In both cases, monomer conversion increased as soon as the rotational speed was lowered and quickly reached a new steady-state value much higher than the pre-

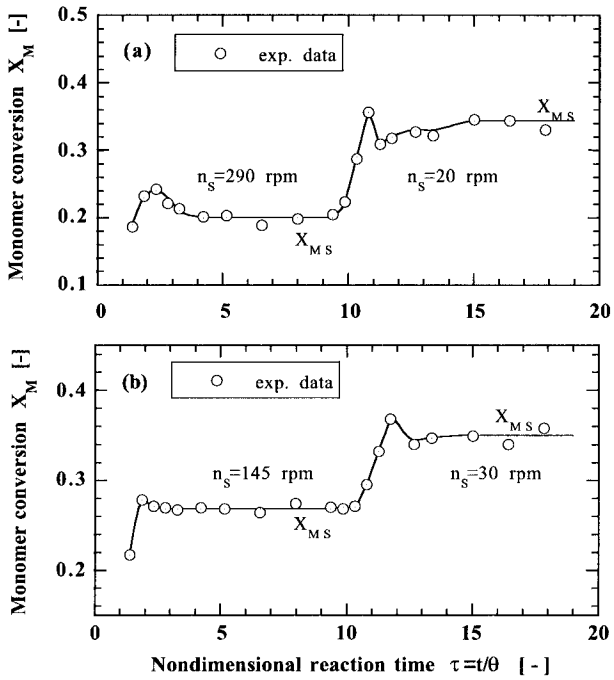

Figure 5 Effect of rotational speed of inner cylinder on steady-state monomer conversion.

vious one, at least in less than twice the reactor mean residence time. The solid lines indicate steady-state monomer conversions. It can be seen that the lower the rotational speed of the inner cylinder, the higher the steady-state monomer conversion.

It can be concluded from these experimental results that a very stable operation is possible when continuous emulsion polymerization of styrene is carried out in a CTVFR and that steady-state monomer conversion and therefore a steady-state number of polymer particles produced can be controlled very easily only by varying the rotational speed of the inner cylinder. These characteristics are very suitable for the prereactor of a continuous emulsion polymerization reactor system with CSTRs connected in series.

Derivation of Mathematical Model for Continuous Emulsion Polymerization of Styrene in a Single CTVFR

Basic Kinetic Equations for Continuous Emulsion Polymerization in CSTRs

By applying the kinetic model proposed previously for the continuous emulsion polymerization of styrene in CSTRs[6] and the tank-in-series model to a CTVFR, a quantitative explanation of the kinetic behavior of the observed continuous nonseeded emulsion polymerization of styrene in a single CTVFR is attempted here.

The elementary reactions of the emulsion polymerization of styrene and their rate expressions are defined in Table II, for which it was assumed that (1) polymer particles are generated from emulsifier micelles and (2) each polymer particle contains at most one radical. When the tank-in-series model was applied to a CTVFR in developing a mathematical model for the continuous emulsion polymerization of styrene in a single CTVFR, as shown in Figure 6, the following assumptions were made: (1) each CSTR is uniformly mixed; (2) the density change in the reaction mixture is negligible; and (3) no polymerization occurs between stages. Based on the elementary reactions and their rate expressions (Table II), we were then able to establish the following equations for each species in the ith reactor stage:

Table II Elementary Reactions in Emulsion Polymerization and Their Rates

Reaction	Reaction Type	Reaction Rate	
Initiation of radicals	$I \rightarrow 2R^*$	$r_i = 2k_d f I_o$	(E1)
Particle formation from micelles	$R^* + m_s \rightarrow N^*$	$k_1 m_s R^*$	(E2)
Initiation	$R^* + N \rightarrow N^*$	$k_2 N R^*$	(E3)
Termination	$R^* + N^* \rightarrow N$	$k_2 N^* R^*$	(E4)
Propagation in particle	$P_j^* + M \rightarrow P_{j+1}^*$	$k_p M_p N^*$	(E5)
Transfer to monomer	$P_j^* + M \rightarrow P_j + M^*$	$k_{mf} M_p N^*$	(E6)
Transfer to transfer agent	$P_j^* + T \rightarrow P_j + T^*$	$k_{Tf} T_p N^*$	(E7)
Desorption of radical from polymer particles	$N^* \rightarrow N + R^*$	$k_f N^*$	(E8)

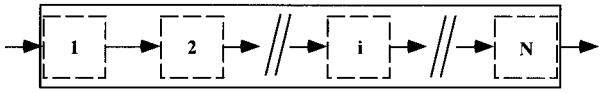

Figure 6 Schematic representation of tank-in-series model applied to a continuous CTVFR.

(A) Initiator concentration, I_i:

$$\theta_i \frac{dI_i}{dt} = I_{i-1} - I_i - k_d f I_i \theta_i \tag{3}$$

where θ_i is the mean residence time in the ith reactor, k_d is the decomposition rate constant for initiator, and f is the initiator efficiency.

(B) Concentration of radicals in the water phase, R_i^*:

$$\theta_i \frac{dR_i^*}{dt} = (r_{ii} + k_{fi} N_i^* - k_1 R_i^* m_{si} - k_2 R_i^* N_{Ti})\theta_i + R_{i-1}^* - R_i^* \tag{4}$$

where r_i is the rate of radical production in the aqueous phase, N^* is the number of active polymer particles containing polymerizing radicals, N_T is the total number of polymer particles, m_s is the number of micelles per unit volume of water, k_1 and k_2 are the rate coefficients for radical entry into micelles and polymer particles, respectively, and k_f is the rate coefficient for radical desorption from polymer particles into the aqueous phase and is, in good approximation, given by[21–23]

$$k_{fi} = \frac{12 D_w \delta C_m}{m_d \bar{d}_{pi}^2} \tag{5}$$

where D_w is the diffusion coefficient of monomer radicals in the aqueous phase, m_d is the partition coefficient of monomer radicals between the polymer particle and aqueous phases, δ is the ratio of water-side resistance to overall mass transfer resistance for monomer radicals, C_m is the chain transfer constant to monomer, and $\bar{d}_{pi}$ is the average diameter of polymer particles at the ith reactor stage and is given by

$$\bar{d}_{pi} = \left[\frac{6}{\pi} \bar{v}_{pi}\right]^{1/3} \tag{6}$$

where $\bar{v}_i$ is the average volume of polymer particles and is given by

$$\bar{v}_{pi} = \frac{M_0 X_{Mi} (1 - \phi_i)^{-1}}{N_{Ti} \bar{\rho}} \tag{7}$$

where ϕ_i is the weight fraction of monomer in polymer particle and $\bar{\rho}$ is the density of monomer-swollen polymer particles. Considering the sufficiently long half-life of potassium persulfate decomposition compared with the reactor mean residence, r_{ii} can be approximated as

$$r_{ii} = r_i = 2 k_d f I_F \tag{8}$$

where I_F is the initiator concentration in the initiator feed stream.

(C) The total number of polymer particles, N_{Ti}:

$$\theta_i \frac{dN_{Ti}}{dt} = k_1 R_i^* m_{si} \theta_i + N_{Ti-1} - N_{Ti} \tag{9}$$

(D) The number of active polymer particles containing a polymerizing radical, N_i^*:

$$\theta_i \frac{dN_i^*}{dt} = k_1 m_{si} R_i^* \theta_i + k_2 N_i R_i^* \theta_i - k_2 N_i^* R_i^* \theta_i - k_{fi} N_i^* \theta_i + N_{i-1}^* - N_i^* \tag{10}$$

where N_i is the number of dead polymer particles containing no radicals.

(E) Monomer concentration, M_i:

$$\theta_i \frac{dM_i}{dt} = M_{i-1} - M_i - \left[\frac{k_p M_{pi} M_g}{N_A}\right] N_i^* \theta_i \tag{11}$$

where k_p is the propagation rate constant, M_g is the molecular weight of monomer, M_{pi} is the monomer concentration in the polymer particles, and N_A is the Avogadro's number.

(F) The concentration of total emulsifier molecules, S_i:

$$\theta_i \frac{dS_i}{dt} = S_{i-1} - S_i \tag{12}$$

$$S_i = S_{mi} + S_{CMC} + (36\pi/a_s^3)^{1/3} \bar{v}_{pi}^{2/3} N_{Ti} \tag{13}$$

where S_m is the concentration of emulsifier forming micelles, S_{CMC} is the critical micellar concentration, and a_s is the surface area occupied by an emulsifier molecule.

Applying the steady-state assumption to eq. (4) produces

$$R_i^* = \frac{r_i + k_{fi} N_i^*}{k_1 m_{si} + k_2 N_{Ti}} = \frac{r_i + k_{fi} N_i^*}{k_1 m_{si} (1 + (\varepsilon N_{Ti}/S_{mi}))} \tag{14}$$

where $S_{mi} = A_n m_{si}$ and $\epsilon = (k_2 S_{mi}/k_1 m_{si}) = (k_2/k_1)A_n$. Here A_n is the aggregation number of emulsifier molecules per micelle and ϵ/A_n indicates the radical capture efficiency of polymer particles relative to micelles. At the present stage, however, we cannot help in determining the value of ϵ experimentally because there are no exact values for k_1, k_2 and A_n in the literature.[6,24,25]

The introduction of eq. (14) into eqs. (9) and (10) and rearrangement yields eqs. (15) and (16), respectively:

$$\theta_i \frac{dN_{Ti}}{dt} = \frac{r_i + k_{fi}N_i^*}{1 + (\varepsilon N_{Ti}/S_{mi})}\,\theta_i + N_{Ti-1} - N_{Ti} \quad (15)$$

$$\theta_i \frac{dN_i^*}{dt} = (r_i + k_{fi}N_i^*)\theta_i\left(1 - \frac{2N_i^*/N_{Ti}}{1 + [1/(\varepsilon N_{Ti}/S_{mi})]}\right) - k_{fi}N_i^*\theta_i + N_{i-1}^* - N_i^* \quad (16)$$

At the reactor stage in which monomer droplets exist ($X_{Mi} \le X_{MC2}$), the monomer concentration in the polymer particles, M_{pi}, is constant and equal to M_{pc}. Considering this, eq. (17a) is produced by introducing $M_i = M_o(1 - X_{Mi})$ into eq. (11).

$$\theta_i \frac{dX_{Mi}}{dt} = X_{Mi-1} - X_{Mi} + KN_i^*\theta_i \quad (17\text{-a})$$

where K is a constant defined by $K = k_p M_{pc} M_g/M_o N_A$.

On the other hand, at the reactor stage in which monomer droplets have already disappeared ($X_{Mi} > X_{MC2}$), it holds that $M_{pi} = M_{pc}(1 - X_{Mi}/1 - X_{MC2})$. Introduction of this expression into eq. (11) yields

$$\theta_i \frac{dX_{Mi}}{dt} = X_{Mi-1} - X_{Mi} + \left(\frac{1 - X_{Mi}}{1 - X_{MC2}}\right)KN_i^*\theta_i \quad (17\text{-b})$$

Considering that at a steady state, $S_i = S_F$ at any stage, eq. (13) can be simplified as

$$S_F = S_{mi} + S_{CMC} + k_v(M_o X_{Mi})^{2/3} N_{Ti}^{1/3} \quad (18)$$

where $k_v = (36\pi/[(1 - \phi_c)^2\, a_s{}^3 \rho^2])^{1/3}$ and ϕ_c denotes the weight fraction of monomer in the polymer particles.

Basic Kinetic Equations for Continuous Emulsion Polymerization in a Single CTVFR

By equating the derivatives of the left-hand side of eqs. (15)–(17b) to zero when a CTVFR is operated in a steady state, we have eqs. (19)–(23), respectively: for the total number of polymer particles, N_{Ti}, at the ith reactor stage

$$N_{Ti} = N_{Ti-1} + \frac{r_i + k_{fi}N_i^*}{1 + (\varepsilon N_{Ti}/S_{mi})}\,\theta_i \quad (19)$$

For the number of active polymer particles, N_i^*, at the ith reactor stage,

$$N_i^* = N_{i-1}^* + (r_i + k_{fi}N_i^*)\theta_i \times \left(1 - \frac{2N_i^*/N_{Ti}}{1 + [1/(\varepsilon N_{Ti}/S_{mi})]}\right) - k_{fi}N_i^*\theta_i \quad (20)$$

At the reactor stage where monomer droplets exist, eq. (17a) becomes

$$X_{Mi} = X_{Mi-1} + KN_i^*\theta_i \quad (21\text{-a})$$

At the reactor stage where no more monomer droplets exist, eq. (17b) becomes

$$X_{Mi} = X_{Mi-1} + \left(\frac{1 - X_{Mi}}{1 - X_{MC2}}\right)KN_i^*\theta_i \quad (21\text{-b})$$

Theoretical values of the steady-state monomer conversion and particle number were obtained as follows: The number of tanks in series, N, corresponding to the CTVFR operated under given conditions was first predicted by eq. (2). Then the stage-to-stage calculations were successively performed from the first to the Nth reactor stage, using a set of simultaneous equations, eqs. (19)–(21).

Values of Numerical Constants Used

The values of the numerical constants used in this study are listed in Table III. Except for the values of parameters δ and ϵ, these values are already known in the literature. In this study, therefore, only the values of these unknown parameters, δ and ϵ, were determined so as to get the best fit between the model predictions and experimental data for batch emulsion polymerization of styrene at 50°C. Figure 7 shows a typical example of the comparison between the experi-

Table III Values of Used Numerical Constants at 50°C

Constants	Unit	Value	Source
k_p	(dm^3/mol sec)	212	Harada et al.[25]
k_df	(1/sec)	6.65×10^{-7}	Harada et al.[25]
C_m	(—)	1.2×10^{-5}	Nomura et al.[26]
D_{wm}	(cm^2/sec)	1.2×10^{-5}	Nomura et al.[26]
m_d	(—)	1300	Nomura et al.[26]
S_{cmc}	(g/dm^3 water)	0.75	This work
M_{pc}	(mol/dm^3 part.)	5.48	Harada et al.[25]
δ	(—)	0.1	This work
ε	(—)	2.3×10^5	This work
a_s	(cm^2/molecule)	36×10^{-16}	Harada et al.[25]
X_{MC2}	(—)	0.43	Harada et al.[25]

mental results[25] and the model predictions obtained by using the values listed in Table III and the basic kinetic equations shown in Table IV, which were derived from eqs. (15)–(17) for batch emulsion polymerization of styrene. Considering these good fits, both the kinetic equations and the values of the numerical constants listed in Table III can be regarded as reasonably applicable to the prediction of the kinetic behavior of the continuous emulsion polymerization of styrene in a single CTVFR at 50°C.

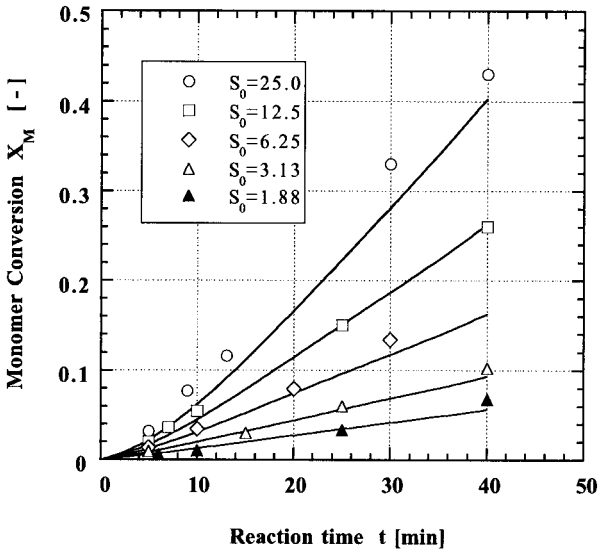

Figure 7 Comparison between model predictions and experimental results on the course of batch emulsion polymerization of styrene (experimental conditions: initiator, I_0 = 1.25 g/dm^3 water; monomer, M_0 = 500 g/dm^3 water; emulsifier, S_0 = 1.88–25.0 g/dm^3 water; 50°C; solid lines = model predictions).

RESULTS AND DISCUSSION

Effects of Operating Variables on Kinetic Behavior of Continuous Emulsion Polymerization of Styrene in a Single CTVFR

Effect of Taylor Number

The effect of the Taylor number on steady-state monomer conversion, X_{MS}, and on the particle number, N_{TS}, was investigated by varying the rotational speed of the inner cylinder, n_S, between 10 and 290 rpm with the emulsifier, monomer, and initiator concentrations in each feed stream fixed at S_F = 6.25 g/dm^3 water, M_F = 100 g/dm^3 water, and I_F = 1.25 g/dm^3 water, respectively. The reactor mean residence was kept at θ = 21.3 min.

Since the viscosity of the reaction mixture comprising a heterogeneous phase changes with the progress of polymerization, it is difficult to calcu-

Table IV Basic Kinetic Equations for Batch Emulsion Polymerization

$$\frac{dN_T}{dt} = \frac{r_i + k_f N^*}{1 + (\varepsilon N_T / S_m)} \tag{B1}$$

$$\frac{dN^*}{dt} = (r_i + k_f N^*)\left(1 - \frac{2N^*/N_T}{1 + [1/(\varepsilon N_T/S_m)]}\right) - k_f N^* \tag{B2}$$

$$\frac{dX_M}{dt} = KN^* \qquad (X_M \le X_{MC2}) \tag{B3-1}$$

$$\frac{dX_M}{dt} = \left(\frac{1 - X_M}{1 - X_{MC2}}\right) KN^* \qquad (X_M > X_{MC2}), \tag{B3-2}$$

late the exact Taylor number. When the Taylor number is calculated, therefore, the viscosity of water at 50°C was employed as an approximate value of the viscosity of the reaction mixture because the volume fraction of the dispersed monomer and polymer phase in the reaction mixture is rather low. For example, the rotational speed of the inner cylinder from 10 to 290 rpm roughly corresponds to Taylor number from 187 to 5420. In this study, therefore, we exclusively used the rotational speed of the inner cylinder as a substitute for the Taylor number.

Including the experimental data points shown in Figure 5, all the observed steady-state monomer conversions, X_{MS}, and the particle numbers, N_{TS}, are plotted against the value of n_S in Figure 8. The keys, open circles in the figures, indicate the experimental data points. The solid lines, on the other hand, represent the model predictions obtained by using eq. (2) and eqs. (19)–(21). It can be seen that with decreasing the rotational speed, the steady-state monomer conversion and particle number increases gradually from a lower limit, approaching an upper limit. The lower limit, shown by a dotted line, corresponds to the values predicted for a single ideal CSTR ($N = 1$), and the upper limit, shown by a broken line, corresponds to those predicted for an ideal PFR ($N = \infty$). Fairly good agreement can be seen between the experimental and predicted values when the rotational speed is faster than 45 rpm. When the rotational speed is 290 rpm, the observed steady-state monomer conversion and particle number also agree fairly well with those predicted for a single ideal CSTR. This indicates that when the rotational speed is 290 rpm, the flow pattern in the CTVFR is already in the region of perfectly mixed flow ($N = 1$). Both the experimental steady-state monomer conversion and particle number become maximum at around 45 rpm and then decrease slightly with a decreasing of the rotational speed. This may be ascribed to the so-called back-mixing induced by monomer droplets rising upward in the annular space because the toroidal motion of fluid elements can no longer hold them inside each cellular vortex against the buoyancy acting on the monomer droplets when the rotational speed of the inner cylinder lowers.

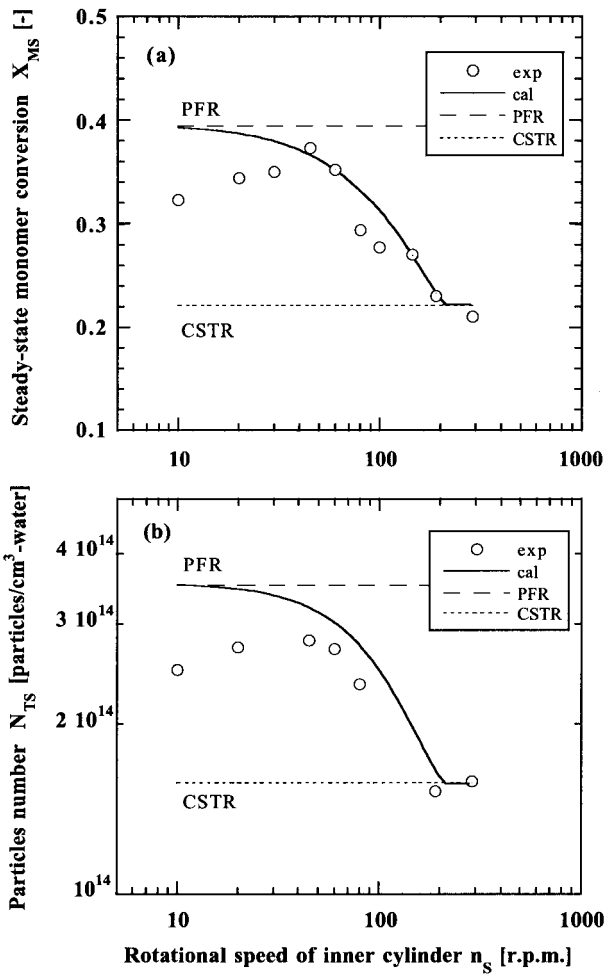

Figure 8 Effect of rotational speed of inner cylinder (Taylor number) on the steady-state monomer conversion and the number of polymer particles and a comparison between the experimental results and model prediction.

Effect of Emulsifier Concentration

The effect of emulsifier concentration on steady-state monomer conversion and particle number was investigated by varying the emulsifier concentration in the emulsion feed stream from S_F = 2–12.5 g/dm^3 water with the monomer concentration in the emulsion feed stream fixed at M_F = 100 g/dm^3 water while the initiator concentration in the initiator feed stream was fixed at I_F = 1.25 g/dm^3 water. The rotational speed and the reactor mean residence time were kept at n_S = 45 rpm and θ = 21.3 min, respectively.

In Figure 9 the observed steady-state monomer conversion, X_{MS}, and the particle number, N_{TS}, are plotted against the emulsifier concentration in the feed stream, S_F. The solid lines represent the predicted values corresponding to the reaction conditions. The chain and dotted lines, on the

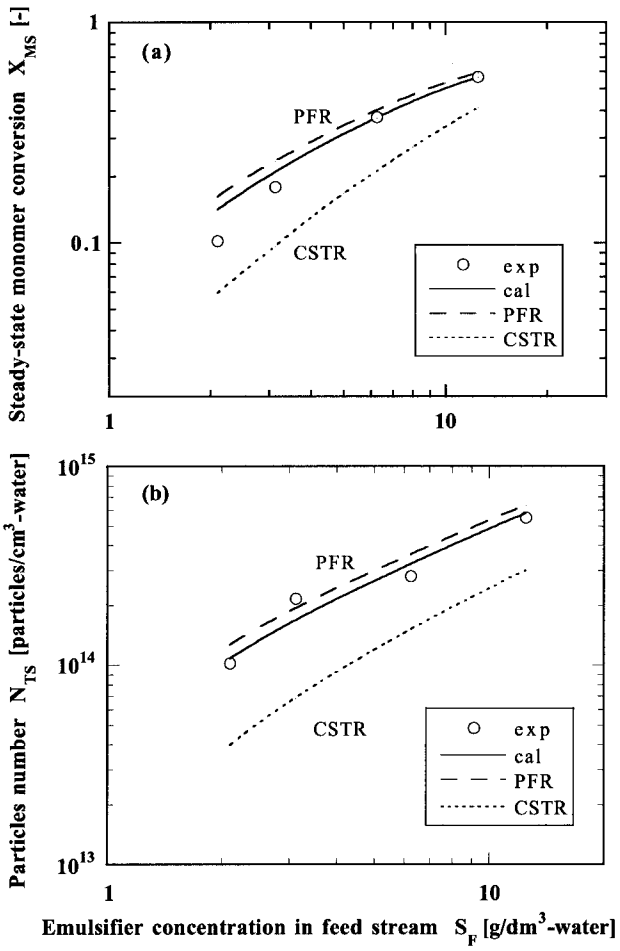

Figure 9 Effect of emulsifier concentration in the feed on the steady-state monomer conversion and the number of polymer particles and a comparison between the experimental results and model prediction.

other hand, show the calculated results for ideal PFR and CSTR, respectively. A fairly good agreement can be seen between the experimental and predicted values. We can conclude, therefore, that the present kinetic model is a good predictor for the effect of emulsifier concentration on the kinetic behavior of continuous emulsion polymerization of styrene in a CTVFR.

Effect of Initiator Concentration

The effect of initiator concentration on steady-state monomer conversion and particle number was investigated by varying the initiator concentration in the initiator feed stream from I_F = 0.313–2.5 g/dm^3 water with the emulsifier and monomer concentrations in the emulsion feed stream fixed at S_F = 6.25 g/dm^3 water and M_F = 100 g/dm^3-water, respectively. The rotational speed and the reactor mean residence time were kept at n_S = 45 rpm and θ = 21.3 min, respectively.

Figure 10 shows the experimental results and compares them with the predicted values. The solid lines represent the calculated values corresponding to the reaction conditions. The chain and dotted lines, on the other hand, show the values predicted for an ideal PFR and CSTR, respectively. The experimental results for the steady-state monomer conversion agree well with the predicted values, while the experimental data on particle number show wide scattering and deviate from the predicted values, possibly because of errors introduced during the measurement of

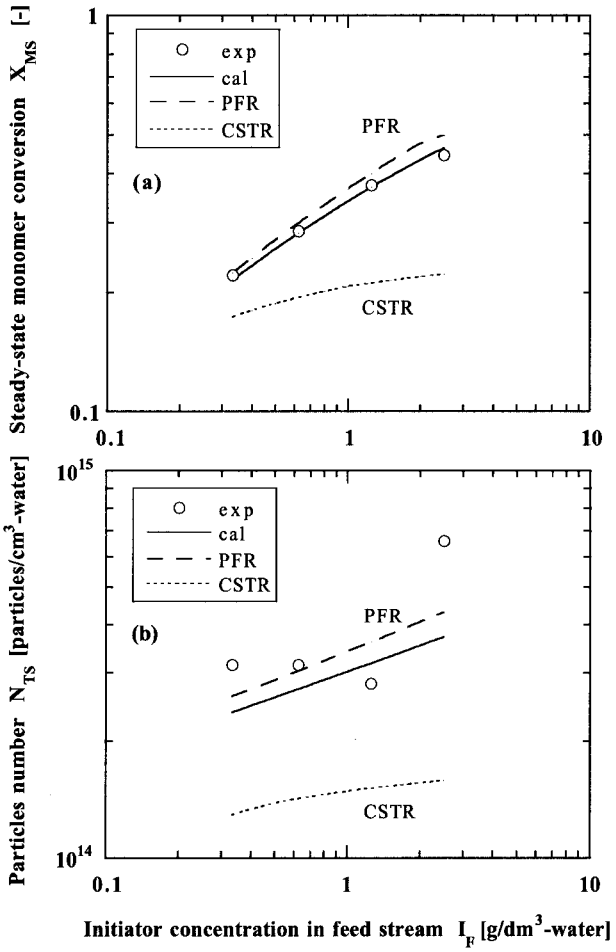

Figure 10 Effect of initiator concentration in the feed on the steady-state monomer conversion and the number of polymer particles and a comparison between the experimental results and model prediction.

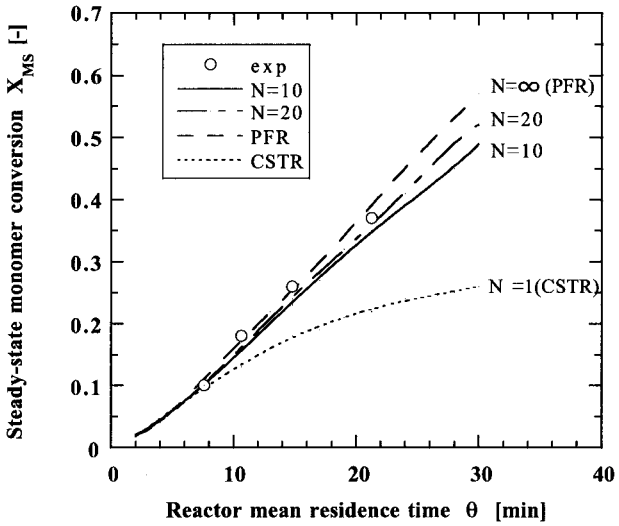

Figure 11 Effect of reactor mean residence time on the steady-state monomer conversion and comparison between the experimental result and model predictions.

volume-average particle diameter by electron microscopy.

Effect of Reactor Mean Residence Time

The effect of reactor mean residence on the steady-state monomer conversion was examined in this experiment with the emulsifier and monomer concentrations in the emulsion feed stream fixed at S_F = 6.25 g/dm^3 water and M_F = 100 g/dm^3 water, respectively, while the initiator concentration in the initiator feed stream was fixed at I_F = 1.25 g/dm^3 water. The rotational speed and the reactor mean residence time were kept at n_S = 45 rpm and θ = 21.3 min, respectively.

Figure 11 shows a plot of the experimental steady-state monomer conversion, X_{MS}, against the reactor mean residence time, θ. The open circles in the figure indicate steady-state monomer conversion. The broken, chain, solid, and dotted lines, on the other hand, show the predicted values corresponding to an ideal PFR ($N = \infty$), 20 and 10 CSTRs in series, and a single ideal CSTR (N = 1), respectively. It can be seen that when the rotational speed is 45 rpm, the observed steady-state monomer conversion increases along the line corresponding to a reactor system with N = 20 CSTRs in series or higher, which is very close to the line for an ideal PFR.

CONCLUSION

We carried out the continuous emulsion polymerization of styrene in a single CTVFR and clarified the effects of emulsifier and initiator concentrations in the feed streams, the rotational speed of the inner cylinder (Taylor number), and the reactor mean residence time on the steady-state monomer conversion and particle number. We found, as expected, that steady-state conversion and particle number can be freely controlled within two limits corresponding to ideal PFR and CSTR only by varying the rotational speed of the inner cylinder. Further, we found that a mathematical model that we developed by combining an empirical correlation of the mixing characteristics of a CTVFR and a kinetic model, proposed previously for the continuous emulsion polymerization of styrene in CSTRs connected in series, could explain the observed kinetic behavior of the continuous emulsion polymerization of styrene in a CTVFR.

Another important characteristic of a CTVFR as a continuous emulsion polymerization reactor is that very stable long-term operation is possible with this reactor without shear-induced coagulation and polymer deposition onto the inner and outer cylinder surfaces. This is because the reaction mixture in a CTVFR is exposed in a low shear field due to the lower rotational speed of the inner cylinder. Considering these characteristics, we can conclude that a CTVFR is very suitable for the first reactor (prereactor), that is, the seeder for a continuous emulsion polymerization reactor system.

REFERENCES

1. Gershberg, D. B.; Longfield, J. E. Presented at the 54th AIChE Annual Meeting, New York, 1961.
2. Sato, T.; Taniyama, I. Kogyo Kagaku Zasshi 1965, 68, 106.
3. Omi, S.; Ueda, T.; Kubota, H. J. Chem Eng Japan 1969, 2, 123.
4. Gerrens, H.; Kuchner, K. Br Polym J 1970, 2, 18.
5. Degraff, A. W.; Poehlein, G. W. J Polym Sci A-2 1971, 9, 1955.
6. Nomura, M.; Harada, M.; Kojima, H.; Eguchi, W.; Nagata, S. J Appl Polym Sci 1971, 15, 675.
7. Ueda, T.; Omi, S.; Kubota, H. J Chem Eng Japan 1971, 4, 50.
8. Brooks, B. W. Br Polym J 1973, 5, 199.

9. Kiparissides, C. MacGregor, J. F.; Hamielec, A. E. Can J Chem Eng 1980, 58, 45.
10. Nomura, M.; Sasaki, S.; Fujita, K.; Harada, M.; Eguchi, W. 180th ACS Meeting, Organic Coatings and Plastics Chemistry, 1980.
11. Nomura, M.; Harada, M. ACS Symposium Series 165; American Chemical Society: Washington, DC, 1981; p 121.
12. Imamura, T.; Saito, K.; Ishikura, S.; Nomura, M.Polym Int 1993, 30, 203.
13. Cohen, S.; Maron, D. M. Chem Eng J 1983, 27, 87.
14. Janes, D. A.; Thomas, N. H.; Callow, J. A. Biotechnol Tech 1987, 1, 257.
15. K. Kataoka, N. Ohmura, M. Kouzu, Y. Simamura, and M. Okubo, Chem Eng Sci 1995, 50, 1409.
16. Kataoka, K.; Doi, H.; Hongo, T. J Chem Eng Japan 1975, 8, 472.
17. Pudjiono, P. I.; Tavare, N. S.; Garside, J.; Nigam, K. D. P. Chem Eng J 1992, 48, 101.
18. Lathrop, D. P.; Fineberg, J.; Swinny, H. L. Phys Rev Lett 1992, 68, 1515.
19. Enokida, Y.; Nakata, K.; Suzuki, A. AIChE J 1989, 35, 1211.
20. Christine, M.; Moore, V.; Cooney, C. L. AIChE J 1995, 41, 723.
21. Harada, M.; Nomura, M.; Eguchi, W.; Nagata, S. J Chem Eng Japan 1971, 4, 54.
22. Nomura, M.; Harada, M. J Appl Polym Sci 1981, 26, 17.
23. Nomura, M. Emulsion Polymerization; Piirma, I., Ed.; Plenum: New York, 1982; p 191.
24. Nomura, M.; Harada, M. ACS Symposium Series 165, American Chemical Society: Washington, DC, 1981; p 121.
25. Harada, M.; Nomura, M.; Kojima, H.; Eguchi, W.; Nagata, S. J Appl Polym Sci 1972, 16, 811.
26. Nomura, M.; Yamamoto, K.; Horie, I.; Fujita, K.; Harada, M. J Appl Polym Sci 1982, 27, 2483.